Iranian Journal of Fuzzy Systems

Volume 23, Number 4, (2026), pp. 121-143

Original paper

Stochastic Koopman operator-based adaptive fuzzy control for nonlinear systems under unmodeled dynamics

M. A. Labbaf Khaniki [1] and E. Moradi [2]

[1] *Faculty of Electrical Engineering, K.N. Toosi University of Technology, Tehran, Iran*
[2] *Department of Electrical Engineering, YI.C., Islamic Azad University, Tehran, Iran*

mohamad95labafkh@gmail.com, ElaheMoradi@iau.ac.ir

Abstract

This paper introduces a novel stochastic Koopman-based adaptive fuzzy control framework that combines Koopman operator theory with Takagi-Sugeno-Kang (TSK) fuzzy logic to effectively manage nonlinear systems under unmodeled dynamics and diverse stochastic disturbances. The core innovation lies in the concurrent online learning of sparse Koopman observables and the fuzzy controller using deep dictionary learning, replacing static feature sets to enhance adaptability significantly. A robust Lyapunov-based stability analysis in the Koopman observable space, supported by linear matrix inequality criteria, guarantees reliable performance across Gaussian and non-Gaussian noise conditions. Simulation results on benchmark systems, including a 4D hyperchaotic system and an inverted pendulum, demonstrate superior tracking accuracy, disturbance rejection, and computational efficiency compared to model predictive control (MPC), Nonlinear model predictive control (NMPC) and classical TSK fuzzy controllers, with the lowest IAE (1.4933, 3.2627) and ISE (2.3226, 5.0745) metrics. The method's balance of interpretability and data-driven modeling makes it ideal for real-time control of complex, uncertain systems. While offering strong theoretical foundations and addressing critical gaps in robustness and scalability, further empirical validation, and enhanced visual representations of the architecture could strengthen its impact. This work advances adaptive fuzzy control and data-driven modeling, with significant potential for applications in robotics, smart infrastructure, and other safety-critical domains.

Keywords: Stochastic Koopman, adaptive fuzzy control, deep dictionary learning, robustness, nonlinear systems.

1 Introduction

Nonlinear control systems lie at the heart of virtually all advanced engineering disciplines today, from robotics and aerospace to autonomous vehicles, renewable energy systems, biomedical devices, and critical infrastructure protection. Unlike linear systems, which admit elegant and globally valid analytical solutions, nonlinear systems exhibit rich, complex behaviors-multiple equilibria, limit cycles, chaos, bifurcations, and extreme sensitivity to initial conditions and parameters-that make precise modeling and control extraordinarily difficult [1]. Yet it is precisely these nonlinear phenomena that govern the majority of real-world dynamical processes engineers seek to command. The ability to reliably control such systems in the presence of significant uncertainty-whether arising from unmodeled dynamics, unknown parameters, external disturbances, or

Corresponding Author: E. Moradi
Received: August 2025; Revised: April 2026; Accepted: July 2026.
https://doi.org/10.22111/ijfs.2026.52890.9350

inherent stochasticity-has become one of the defining challenges of twenty-first-century control theory and, by extension, of technological progress itself [21]. In autonomous aerial vehicles, unmodeled aerodynamic effects and sudden wind gusts can rapidly destabilize flight if the controller cannot adapt in real time. In modern power grids integrating large amounts of intermittent renewable generation, unpredictable load fluctuations and stochastic renewable injection create voltage and frequency deviations that classical linear controllers struggle to contain [24]. In surgical robotics, unmodeled tissue stiffness variations and physiological tremors demand controllers that remain stable and precise under distributional shifts that no offline model can fully anticipate.

Classical control theory, built largely on linearization around operating points, superposition, and frequency-domain tools, inevitably falters when the operating regime shifts far from the linearization point or when high-order nonlinearities dominate [6]. Even sophisticated nonlinear techniques such as feedback linearization, backstepping, or sliding-mode control typically require an accurate analytical model of the system-a luxury rarely available in practice. Unmodeled dynamics (neglected high-frequency modes, actuator nonlinearities, parameter drift, or entirely unknown interaction terms) and stochastic disturbances (sensor noise, environmental randomness, or unpredictable human inputs) compound the difficulty, often leading to performance degradation or outright instability [43]. In high-dimensional systems—common in robotics, power networks, and autonomous swarms—the curse of dimensionality renders many traditional methods computationally prohibitive, while the lack of interpretability in black-box approaches raises serious barriers to certification and deployment in safety-critical applications.

Over the past two decades, two particularly promising data-driven paradigms have emerged to address subsets of these challenges: Koopman operator theory and adaptive fuzzy control. Koopman theory offers an elegant solution to the core problem of nonlinearity by lifting the state space into a higher- (often infinite-) dimensional space of observables in which the nonlinear dynamics become linear [38]. When a suitable set of observables is found, the infinite-dimensional Koopman operator can be approximated by a finite-dimensional matrix using methods such as Extended or Randomized Dynamic Mode Decomposition (EDMD, RDMD) or deep-learning-based autoencoders. The resulting linear representation enables the application of powerful linear control tools-LQR [47], model predictive control, robustness analysis via μ-synthesis, etc.—to fundamentally nonlinear systems [31]. However, virtually all existing Koopman-based control approaches rely on a fixed, pre-selected dictionary of observables (polynomials, radial basis functions, neural network features, etc.).

Adaptive fuzzy control, particularly Type-2 and Takagi-Sugeno-Kang (TSK) fuzzy systems, has meanwhile established itself as a powerful framework for handling both nonlinearity and linguistic uncertainty through human-interpretable rules and online parameter adaptation [7]. Fuzzy controllers excel at approximating unknown nonlinear functions universally and at incorporating expert knowledge when available [11]. Yet traditional adaptive fuzzy schemes suffer from three critical limitations that prevent them from fully addressing modern control challenges: (i) most adapt only the consequent parameters while keeping the premise structure and membership functions fixed, limiting their ability to restructure knowledge under distributional shift; (ii) they rarely incorporate explicit stochastic modeling or higher-order moment constraints, leaving them vulnerable to heavy-tailed or non-Gaussian disturbances; and (iii) rigorous stability proofs in the presence of both approximation errors and stochastic noise remain scarce, especially for high-dimensional systems [28].

Perhaps more fundamentally, these two paradigms-Koopman linearization and adaptive fuzzy control-have evolved almost entirely in parallel, with remarkably little cross-fertilization despite their complementary strengths. Koopman methods provide global linear embeddings but struggle with time-varying or uncertain dynamics when the observable dictionary is static. Fuzzy systems offer unparalleled flexibility and interpretability in approximating unknown nonlinearities but lack a principled way to embed the dynamics into a linear representation amenable to optimal control and formal stability analysis. Bridging this divide holds the promise of a new generation of simultaneous controllers data-efficient, provably stable, robust to stochastic and distributional uncertainty, computationally scalable, and linguistically interpretable-precisely the characteristics demanded by next-generation autonomous and cyber-physical systems [9].

This paper directly addresses these fundamental challenges—namely, the inability of static models to capture evolving unmodeled dynamics and the vulnerability of classical controllers to complex noise—by proposing a unified, two-level adaptive framework. We introduce the **Adaptive Stochastic Koopman Fuzzy Control (ASK-FC)** architecture, which establishes a dynamic co-learning loop between a data-driven system identifier and an interpretable rule-based controller. At the lower-level identification tier, we implement a deep dictionary learning network to approximate the Koopman operator. Unlike traditional Koopman methodologies that rely on a fixed, pre-selected basis of functions (such as arbitrary polynomials or static radial basis functions), our network continuously learns and updates a sparse, time-varying set of Koopman observables. This dynamic lifting process identifies the optimal coordinate transformations required to linearize under-lying nonlinear dynamics globally . By doing so, it continuously adapts to structural model mismatches, unmodeled physical effects, and shifting disturbance statistics that would otherwise degrade a static model. Operating simultaneously at the upper-level control tier is a probabilistic Takagi-Sugeno-Kang (TSK) fuzzy controller. Crucially, this controller calculates its actions directly within the linearized, high-dimensional observable space rather than the original highly nonlinear state space. To guarantee real-time adaptability under distributional shifts, both the premise parameters (the Gaussian membership functions dictating the geometric boundaries of the rules) and the consequent parameters (the local linear models dictating the control output) are updated online. This continuous tuning is driven by stochastic gradient descent, which minimizes an instantaneously linearized regret metric tied to the system's closed-loop tracking performance. These two distinct tiers are tightly coupled through a joint optimization objective. This unified loss function actively balances three critical goals: enforcing sparsity in the observable dictionary to prevent computational bottlenecks, minimizing prediction error in the stochastic Koopman matrix estimate, and maximizing physical control accuracy. Furthermore, to explicitly combat severe external uncertainties, the framework integrates an online running covariance estimator. This estimator dynamically tracks higher-order statistical moments of the disturbances. By feeding this real-time statistical data directly into both the observable mapping process and the fuzzy inference engine, the ASK-FC framework actively compensates for complex, non-Gaussian, and heavy-tailed noise profiles that typically destabilize conventional Kalman-based or deterministic controllers.

Ultimately, the proposed ASK-FC framework delivers four breakthrough capabilities that close long-standing gaps in the nonlinear control literature:

- **Integrated Observable and Controller Co-Learning**: A novel paradigm that abandons isolated, two-step control designs. By concurrently learning sparse Koopman observables and adapting a TSK fuzzy controller via deep dictionary learning, the system overcomes the restrictive constraints of fixed basis functions and manually tuned rule bases.

- **Active Robustness to Stochastic Disturbances**: The deployment of a weighted TSK fuzzy model augmented with explicit stochastic perturbation handling. By integrating online covariance adaptation, the controller dynamically reshapes its receptive fields to absorb distributional uncertainty and non-Gaussian noise.

- **Rigorous Probabilistic Stability Guarantees**: The establishment of a Lyapunov-based stability framework evaluated directly within the lifted Koopman observable space. By incorporating higher-order moment constraints and linear matrix inequality criteria, the framework provides mathematically rigorous certificates of robustness even in highly nonstationary environments.

- **Scalable and Interpretable Architecture**: A computationally efficient control design achieved through L_1-regularized dynamic rule sparsification. This approach preserves the linguistic interpretability of fuzzy logic while drastically reducing the computational burden, making it exceptionally suited for high-dimensional, real-time, and safety-critical applications.

The remainder of this paper is organized as follows: Section 2 reviews related work and surveys the relevant literature. Section 3 presents the proposed methodology, encompassing observable learning, fuzzy controller design, online adaptation, and stability analysis. Section 4 discusses simulation results, performance evaluation, implications, and limitations. Finally, Section 5 concludes the paper and suggests directions for future research.

2 Related work

2.1 Foundational work in nonlinear control and Koopman theory

The study of nonlinear control systems has evolved significantly since the introduction of Lyapunov-based methods, which provide rigorous stability guarantees for deterministic systems. Foundational work by Khalil [14] introduced techniques for analyzing nonlinear dynamics, emphasizing the use of Lyapunov functions to ensure stability under bounded disturbances. Simultaneously, fuzzy control emerged as a practical tool for managing nonlinearities, beginning with Zadeh's seminal work on fuzzy logic [44], which introduced interpretable and flexible rule-based systems. The development of TSK fuzzy models by TSK [34] further advanced the field by blending fuzzy logic with local linear models, achieving a balance between interpretability and control performance. Parallel to these efforts, Koopman operator theory—rooted in von Neumann's early work [18]—offered a powerful framework for transforming nonlinear dynamics into a linear representation in a higher-dimensional observable space. This enabled the application of linear control techniques to inherently nonlinear systems. While these foundational contributions laid the groundwork for modern nonlinear control, they generally assumed known system dynamics and stationary environments, limiting their applicability in scenarios involving unmodeled dynamics or stochastic disturbances. [5] presents a theoretically sound and practically efficient data-driven robust NMPC framework that elegantly bounds Koopman approximation errors as polytopic uncertainties, achieving strong stability guarantees and real-time feasibility on nonlinear benchmarks.[13] S. T. Hesarkuchak et al. propose a learning-based approach for Pareto optimal control specifically tailored for large-scale systems with unknown slow dynamics. This paper [15] presents a delay-scheduled adaptive observer-based control strategy that uses a Lyapunov–Krasovskii functional and linear matrix inequalities to achieve robust stabilization of nonlinear systems with time-varying delays, where the observer gain is dynamically adjusted according to the instantaneous delay. This paper [32] proposes a design strategies based on linear programming and Lyapunov stability theory to achieve both stabilization and output tracking for positive singular systems, with the tracking problem solved via a proportional–integral controller that ensures non-negative state trajectories.

2.2 Recent advances in Koopman-based and fuzzy control

Recent advances have increasingly emphasized data-driven and adaptive techniques to manage unmodeled dynamics and stochastic uncertainty. EDMD, introduced by Williams et al. [38], has become a core method for approximating Koopman operators using data-driven observables, enabling control in the lifted linear space. For example, Korda and Mezić [19] applied EDMD to the control of nonlinear systems such as robotic manipulators, demonstrating improved performance over classical methods. However, their approach relies on fixed basis functions—such as polynomials or Fourier modes—that limit adaptability to dynamic environments. Deep learning-based Koopman methods, like [40], have improved the expressiveness of learned observables via neural networks, but often at the expense of interpretability and computational efficiency. A Koopman-based residual modeling approach for the control of a soft robot arm combines a physics-based Koopman model with a data-driven residual to create a linear, data-efficient, and generalizable model that improves control accuracy and real-time applicability for soft robots compared to purely physics-based or purely data-driven methods [4]. In [33], Koopman-based feedback design guarantees exponential stability for nonlinear systems using data-driven methods and robust control grounded in Koopman operator theory. In the fuzzy control domain, Zhang et al. [46] extended TSK models with online parameter tuning, enhancing robustness in tasks such as autonomous vehicle control. However, these models lack mechanisms to adapt the underlying dynamic structure, reducing their responsiveness to evolving system behavior. Observer-based periodic event-triggered adaptive fuzzy control ensures efficient, stable control of nonlinear networked systems by combining state observation, fuzzy adaptation, and event-triggered updates [48] . A cognitive method is proposed in [35] to synthesize fuzzy controller mathematical models using genetic algorithms for tuning, enabling automated, optimized controller design through intelligent search and adaptation. These developments underscore the potential of combining data-driven and rule-based approaches but fall short of simultaneously addressing unmodeled dynamics and stochastic disturbances. Leventides et al. [22] provide an early and inspiring proof-of-concept showing that Koopman operator theory combined with EDMD can successfully linearize and control highly nonlinear hyperchaotic financial systems. This article [3] proposes a cellular teaching-learning-based optimization algorithm designed to effectively track moving optima and solve dynamic multi-objective problems. [23] utilizes interpretable machine learning techniques to develop transparent predictive models for startup success, focusing on funding acquisition, patenting activity, and exit outcomes. This study [30] proposes a comprehensive optimization framework to improve the efficiency of financial resource allocation specifically for scaling businesses. This study [12] develops a vehicle intrusion detection system for highway work zones by integrating inertial sensor data with lightweight deep learning models. This paper [37] develops an optimal control framework for an additive manufacturing supply chain that incorporates waste recycling, deriving time-varying production and recycling policies to minimize total cost while ensuring material flow balance and inventory stability. This paper [45] proposes a proportional–integral fading observer that achieves robust consensus for linear multi-agent systems subject to external disturbances, where the observer's fading memory property effectively attenuates the effect of past measurement noise while the integral action ensures zero steady-state error. This paper [17] proposes a risk-averse next-best-view optimization framework for active path planning that sequentially selects sensing viewpoints to minimize worst-case uncertainty, enabling robust autonomous exploration and mapping under adversarial environmental conditions. This paper [16] proposes a conflict-aware active perception and control framework that integrates control barrier functions with 3D Gaussian Splatting to jointly optimize information gain and safety constraints, enabling a robot to resolve trade-offs between perception-driven exploration and collision-avoidance in real-time. This paper [25] conducts a systematic machine-learning performance study to optimize Flamelet Generated Manifold (FGM) models for turbulent combustion, evaluating various regression techniques to accelerate chemistry integration while maintaining predictive accuracy for species and temperature fields. This paper [2] presents a machine learning-based framework for classifying hardware Trojans, evaluating the importance of various features and comparing multiple classification models to identify the most effective approach for detecting malicious modifications in integrated circuits with high accuracy and low false-positive rates. This paper [29] proposes a reinforcement learning-based framework for sequential load restoration in transmission networks that incorporates human-centered fairness metrics, enabling the agent to learn optimal restoration sequences that balance grid stability, load criticality, and equitable power distribution while satisfying operational constraints via optimal power flow.

2.3 Adaptive and stochastic control approaches

Adaptive and stochastic control strategies have also been explored to tackle uncertainties in nonlinear systems. The paper introduces a fast stochastic MPC method for high-dimensional systems using scenario-based optimization and parallel computing to achieve real-time performance. [26]. Techniques such as particle filters and Bayesian estimation have been employed to manage stochastic disturbances; Gordon et al.[10], for instance, used them to track time-varying noise in dynamic systems. Nevertheless, these methods often presume Gaussian noise, reducing robustness when faced with distributional ambiguity. In fuzzy systems, online adaptation strategies-such as those proposed by Wang et al. [36]-updated membership functions in real time, improving performance in nonstationary environments. Yet, they failed to incorporate data-driven modeling of system dynamics. Likewise, stochastic Koopman methods like those developed by Proctor et al. [27] introduced probabilistic stability guarantees but were constrained by their use of static observables, limiting adaptability to evolving conditions. Data-driven methods and adaptive control use stochastic analysis to model, learn, and control uncertain systems efficiently, improving robustness and optimality in dynamic environments [20]. An adaptive distributed stochastic deep reinforcement learning control strategy is proposed in [8] effectively restores voltage and frequency in islanded AC microgrids despite communication noise and delay. It optimizes secondary control by dynamically adapting to uncertainties and achieving robust performance in a decentralized setting. [39] Propose an adaptive predefined-time control for stochastic switched nonlinear systems that ensures system stability within a fixed time despite full-state error constraints and input quantization effects. [42] Develop a distributionally robust optimal control strategy for nonlinear switched batch processes by lifting the dynamics via the Koopman operator and modeling parametric uncertainty through moment bounds, yielding tractable semidefinite programming formulations with probabilistic performance guarantees. Reference [41] presents an innovative hybrid framework that leverages deep learning-based Koopman operator theory to accurately predict gas concentrations and employs a Fuzzy-PID controller to dynamically optimize ventilation systems in deep coal mines. By integrating data-driven predictive modeling with adaptive rule-based control, the approach successfully manages highly nonlinear environmental dynamics to significantly enhance both underground safety and operational energy efficiency.

This paper [49] develops an observer-based consensus protocol for linear multi-agent systems that achieves leader-follower synchronization under intermittent communication and external disturbances by integrating a robust observer that compensates for both missing data and unknown inputs while ensuring closed-loop stability via Lyapunov analysis.

2.4 Gaps and motivation for the proposed study

Despite substantial advances in data-driven control, three critical gaps persist that motivate the present work. First, virtually all Koopman-based methods rely on pre-specified or hand-crafted observables, rendering them brittle when the system exhibits unmodeled, time-varying, or abruptly changing dynamics—precisely the conditions encountered in safety-critical applications such as autonomous vehicles and power grids. Second, conventional adaptive fuzzy controllers adjust only rule consequents or membership parameters in the original state space, forcing them to compensate for the full nonlinearity from scratch; this leads to slow convergence, high rule complexity, and fragility to hidden or drifting dynamics. Third, rigorous probabilistic stability guarantees under nonstationary stochastic disturbances remain scarce, with most adaptive MPC and stochastic Koopman frameworks offering only empirical robustness or weak boundedness results. To overcome these limitations, we introduce a co-adaptive architecture in which the stochastic Koopman operator and the fuzzy inference system continuously refine each other in a physically meaningful way. The Koopman layer discovers and linearizes the dominant nonlinear modes, transforming structured epistemic uncertainty (unknown functional form) into largely unstructured aleatoric residuals. The fuzzy controller, now operating in this nearly linear lifted space, needs only localized corrections, automatically widening its receptive fields and exploration exactly where the current Koopman embedding is inaccurate. The shared prediction residual simultaneously reshapes the observable geometry and sharpens the fuzzy partition, creating a self-reinforcing loop that progressively reduces both sources of uncertainty. This intimate, bidirectional interaction—absent in all prior Koopman, fuzzy, or hybrid approaches—delivers interpretable rules, strong probabilistic stability certificates, and smooth transition from conservative early-phase robustness to near-optimal terminal performance, as detailed in the following sections.

3 Proposed methodology

The proposed methodology introduces a two-level adaptive architecture that integrates stochastic Koopman operator theory with adaptive fuzzy control to address the challenges of unmodeled dynamics and stochastic disturbances in nonlinear systems. Unlike classical fuzzy control, which adapts only rule weights, our approach simultaneously learns a sparse set of Koopman observables and a fuzzy controller in the lifted observable space, enabling robust, interpretable, and adaptive regulation under distributional ambiguity.

3.1 Koopman observable learning

To capture the latent linear structure of the nonlinear system described by:

$$x_{t+1} = f(x_t, u_t) + w_t, \quad w_t \sim \mathcal{W}, \tag{1}$$

we employ EDMD augmented with deep dictionary learning to identify a sparse set of observables $\{\phi_j\}_{j=1}^k$. Let $\Phi(x) = [\phi_1(x), \ldots, \phi_k(x)]^\top \in \mathbb{R}^k$ be the observable vector. The stochastic Koopman operator is approximated by a finite-dimensional matrix $K \in \mathbb{R}^{k\times k}$ such that:

$$\Phi(x_{t+1}) \approx K\Phi(x_t) + Bu_t + \eta_t, \tag{2}$$

where $B \in \mathbb{R}^{k\times m}$ is the control matrix, and $\eta_t \sim \mathcal{N}(0, \Sigma)$ accounts for stochastic disturbances. The matrices K and B are estimated by solving the least-squares problem:

$$\min_{K,B} \mathbb{E}\left[\sum_{t=0}^{T} \|\Phi(x_{t+1}) - K\Phi(x_t) - Bu_t\|_2^2\right] + \lambda_K\|K\|_F^2 + \lambda_B\|B\|_F^2, \tag{3}$$

where $\lambda_K, \lambda_B > 0$ are regularization parameters to prevent overfitting, and $\| \cdot \|_F$ denotes the Frobenius norm. The data triples $\{(x_t, u_t, x_{t+1})\}_{t=0}^{T-1}$ are collected from system trajectories. To ensure sparsity and expressiveness, we parameterize $\Phi(x)$ using a deep neural network with a sparse dictionary layer:

$$\Phi(x) = W_\ell \sigma(W_{\ell-1}\sigma(\dots \sigma(W_1 x + b_1)\dots) + b_{\ell-1}) + b_\ell, \tag{4}$$

where σ is a nonlinear activation (e.g., ReLU), W_i, b_i are weights and biases, and W_ℓ is constrained via an ℓ_1 penalty to promote sparsity:

$$\min_{W_\ell} \|\Phi(x) - \Phi_{\text{true}}(x)\|_2^2 + \lambda_\Phi \|W_\ell\|_1, \tag{5}$$

where $\lambda_\Phi > 0$ controls sparsity. To enhance robustness, we introduce a kernel-based regularization term to ensure smoothness in the observable space:

$$R_{\text{kernel}}(\Phi) = \sum_{i,j=1}^{N} k(x_i, x_j)\|\Phi(x_i) - \Phi(x_j)\|_2^2, \tag{6}$$

where $k(x_i, x_j) = \exp\left(-\frac{\|x_i - x_j\|_2^2}{\sigma_k^2}\right)$ is a Gaussian kernel with bandwidth σ_k. This approach extends traditional EDMD by learning data-driven observables that capture unmodeled dynamics, addressing the gap in prior work where fixed basis functions (e.g., polynomials, Fourier modes) limit adaptability. The solution to (4) is derived as follows. Define the data matrices $X = [x_0, \dots, x_{T-1}]$, $U = [u_0, \dots, u_{T-1}]$, and $\Phi_X = [\Phi(x_0), \dots, \Phi(x_{T-1})]$. The closed-form solution for K and B is:

$$[K, B] = \left(\Phi_X^+ (\Phi_X \Phi_X^\top + \lambda_K I)^{-1} (\Phi_X U^\top + \lambda_B I)\right), \tag{7}$$

where $\Phi_X^+ = [\Phi(x_1), \dots, \Phi(x_T)]$ is the observable matrix for the next states. This formulation ensures numerical stability and scalability for high-dimensional systems.

3.2 Fuzzy controller design

The fuzzy controller F operates in the Koopman observable space, leveraging the approximately linear dynamics to design interpretable and robust control rules. To explicitly account for uncertainty and unmodeled nonlinearities in the observable space, we adopt a robust, stochastically perturbed TSK fuzzy model. The control action is defined directly as:

$$u_t = \sum_{i=1}^{M} \mu_i(\Phi(x_t)) \cdot (A_i \Phi(x_t) + b_i + \epsilon_i \xi_t), \tag{8}$$

where $\xi_t \sim \mathcal{N}(0, I)$ is a stochastic perturbation, and $\epsilon_i > 0$ is a robustness parameter tuned to balance exploration and stability. The term $\mu_i(\Phi(x_t)) \in [0, 1]$ represents the normalized membership degree for the i-th rule, satisfying $\sum_{i=1}^{M} \mu_i = 1$. The membership functions are Gaussian:

$$\mu_i(\Phi(x_t)) = \frac{\exp\left(-\|\Phi(x_t) - c_i\|_{\Sigma_i^{-1}}^2\right)}{\sum_{j=1}^{M} \exp\left(-\|\Phi(x_t) - c_j\|_{\Sigma_j^{-1}}^2\right)}, \tag{9}$$

where $c_i \in \mathbb{R}^k$ and $\Sigma_i \in \mathbb{R}^{k \times k}$ are the center and covariance matrix of the i-th rule, and $\theta = \{A_i, b_i, c_i, \Sigma_i\}_{i=1}^{M}$ are the fuzzy parameters. The covariance Σ_i is adapted online to reflect the uncertainty in $\Phi(x_t)$:

$$\Sigma_i^{t+1} = \Sigma_i^t + \alpha\left[(\Phi(x_t) - c_i)(\Phi(x_t) - c_i)^\top - \Sigma_i^t\right], \tag{10}$$

where $\alpha \in (0, 1)$ is a learning rate. This formulation allows the controller to exploit the linear structure of the Koopman space while adapting to unmodeled dynamics, addressing the limitations of state-space fuzzy systems that lack robustness to latent nonlinearities.

3.3 Stability analysis

The proposed stochastic Koopman operator-based adaptive fuzzy control system ensures closed-loop stability through probabilistic guarantees derived using Lyapunov theory in the observable space.

Assumption 1 [Lipschitz Dynamics]: The system dynamics $f(x, u, t)$ are Lipschitz continuous in x, i.e., there exists a constant $L > 0$ such that:

$$\|f(x, u, t) - f(y, u, t)\|_2 \le L\|x - y\|_2. \tag{11}$$

Assumption 2 [Bounded Disturbance and Control Uncertainty]: The process noise $\eta_t \sim \mathcal{N}(0, \Sigma)$ and the control perturbation $\xi_t \sim \mathcal{N}(0, I)$ are bounded such that $\mathbb{E}[\|\eta_t\|_2^2] \le \delta_\eta$ and $\sum_{i=1}^{M} \mu_i^2(t)\epsilon_i^2 \le \delta_\xi$ for known constants $\delta_\eta, \delta_\xi > 0$.

Assumption 3 [Bounded Operators]: The Koopman operator K and control matrix B satisfy $\|K\|_{L_2} \le \beta_K$ and $\|B\|_{L_2} \le \beta_B$.

Assumption 4 [Lipschitz Membership]: The fuzzy membership functions $\mu_i(\Phi(x_t))$ are Lipschitz continuous with constant $L_\mu > 0$.

Definition 1 [Lifted Lyapunov Function]: The Lyapunov function in the Koopman observable space is defined as $V(\Phi(x_t)) = \Phi(x_t)^\top P \Phi(x_t)$ with $P \succ 0$. The system is probabilistically stable if the expected Lyapunov difference satisfies:

$$\mathbb{E}[V(\Phi(x_{t+1})) \mid \Phi(x_t), u_t] \le V(\Phi(x_t)) - \gamma\|\Phi(x_t)\|_2^2, \quad \gamma > 0. \tag{12}$$

Lemma 1 [Second-Moment Lyapunov Decrease]: Substituting the robust fuzzy control law into the Koopman approximation, the expected Lyapunov function evaluates to:

$$\begin{aligned}\mathbb{E}[V(\Phi(x_{t+1}))] &= \Phi(x_t)^\top \bar{A}^\top P \bar{A} \Phi(x_t) + 2\Phi(x_t)^\top \bar{A}^\top P B \sum_{i=1}^{M} \mu_i b_i \\ &\quad + \left(\sum_{i=1}^{M} \mu_i b_i\right)^\top B^\top P B \left(\sum_{i=1}^{M} \mu_i b_i\right) + \operatorname{trace}(P(\Delta + \Sigma)),\end{aligned} \tag{13}$$

where $\bar{A} = K + B\sum_{i=1}^{M} \mu_i A_i$ and $\Delta = B\left(\sum_{i=1}^{M} \mu_i^2 \epsilon_i^2\right) I B^\top$. The decrease condition is satisfied, guaranteeing probabilistic stability, if $\bar{A}^\top P \bar{A} - P + \gamma I \prec 0$, the stochastic bounds from Assumption 2 hold, and the linear bias terms remain bounded by a constant β.

3.4 Online stochastic adaptation laws

To ensure simultaneous refinement of the Koopman observables and the fuzzy controller parameters while preserving closed-loop stability, we derive parameter adaptation laws by direct minimization of the expected one-step Lyapunov decrement in the lifted observable space. Consider the quadratic Lyapunov function introduced in Definition 1:

$$V(\Phi(x_t)) = \Phi(x_t)^\top P \Phi(x_t), \quad P \succ 0. \tag{14}$$

After applying control input u_t, the realized observable at the next time step is $\Phi(x_{t+1})$. Define the lifted prediction error (residual) as

$$e_{t+1} = \Phi(x_{t+1}) - K\Phi(x_t) - Bu_t. \tag{15}$$

This residual captures both unmodeled dynamics and the stochastic disturbance η_t in the observable space. The realized (stochastic) Lyapunov increment is

$$\Delta V_t = V(\Phi(x_{t+1})) - V(\Phi(x_t)) = \|K\Phi(x_t) + Bu_t + e_{t+1}\|_P^2 - \|\Phi(x_t)\|_P^2. \tag{16}$$

We construct parameter update laws as normalized stochastic gradients of the regularized instantaneous Lyapunov increment

$$L_t = \Delta V_t + \gamma\|\Phi(x_t)\|_2^2, \tag{17}$$

with projection onto compact convex sets to satisfy the persistent-excitation and boundedness assumptions required for rigorous convergence proofs. Let $\theta = \{A_i, b_i, c_i, \Sigma_i\}_{i=1}^{M}$ denote the fuzzy controller parameters and $W = \{W_j, b_j\}_{j=1}^{\ell}$ the deep dictionary weights parameterizing the observable map $\Phi(x; W)$. The resulting online adaptation laws are as follows.

3.4.1 Adaptation of TSK consequent parameters A_i and b_i

The gradients of L_t with respect to the linear consequent parameters yield

$$\frac{\partial L_t}{\partial A_i} = 2\mu_i(\Phi(x_t))(K\Phi(x_t) + Bu_t + e_{t+1})^\top PB\Phi(x_t)^\top, \tag{18}$$

$$\frac{\partial L_t}{\partial b_i} = 2\mu_i(\Phi(x_t))(K\Phi(x_t) + Bu_t + e_{t+1})^\top PB. \tag{19}$$

The normalized stochastic gradient updates with projection $\mathcal{P}[\cdot]$ are

$$A_i^{t+1} = \mathcal{P}\left[A_i^t - \frac{\gamma_A \mu_i(\Phi(x_t))}{1 + \|\Phi(x_t)\|_2^2}\Phi(x_t)\left(B^\top P e_{t+1}\right)^\top\right], \tag{20}$$

$$b_i^{t+1} = \mathcal{P}\left[b_i^t - \frac{\gamma_b \mu_i(\Phi(x_t))}{1 + \|\Phi(x_t)\|_2^2}B^\top P e_{t+1}\right], \tag{21}$$

where $\gamma_A > 0$ and $\gamma_b > 0$ are adaptation gains.

3.4.2 Adaptation of Gaussian antecedent parameters c_i and Σ_i

The centers and covariances are updated to reduce clustering uncertainty and improve firing-strength accuracy:

$$c_i^{t+1} = \mathcal{P}\left[c_i^t + \gamma_c \mu_i(\Phi(x_t))(\Sigma_i^t)^{-1}(\Phi(x_t) - c_i^t)\left(e_{t+1}^\top P B u_t\right)\right], \tag{22}$$

$$\Sigma_i^{t+1} = \mathcal{P}\left[\Sigma_i^t + \gamma_\Sigma \mu_i(\Phi(x_t))\left((\Phi(x_t) - c_i^t)(\Phi(x_t) - c_i^t)^\top - \Sigma_i^t\right)\right], \tag{23}$$

with $\gamma_c > 0$ and $\gamma_\Sigma \in (0, 1)$. Equation (23) corresponds to an exponentially weighted moving covariance estimate that naturally emerges from Lyapunov-based optimization of the fuzzy partitioning.

3.4.3 Adaptation of Koopman observable mapping $\Phi(x; W)$

The deep dictionary weights W are adapted by backpropagating the residual-driven Lyapunov gradient through the current observable evaluation:

$$\frac{\partial L_t}{\partial W} = 2e_{t+1}^\top P \cdot \frac{\partial \Phi(x_t)}{\partial W}\Big|_{W^t} - 2\Phi(x_t)^\top P \cdot \frac{\partial (K\Phi(x_t))}{\partial W}\Big|_{W^t}. \tag{24}$$

The dominant and stability-preserving term is the residual component, yielding the update

$$W^{t+1} = \mathcal{P}\left[W^t - \gamma_\Phi\left(e_{t+1}^\top P\right)\frac{\partial \Phi(x_t; W)}{\partial W}\Big|_{W^t}\right], \tag{25}$$

where $\gamma_\Phi > 0$ is the dictionary learning rate. This rule performs online P-weighted EDMD in the output layer while allowing deeper layers to adjust the lifting geometry.

3.4.4 Periodic Re-estimation of Koopman matrices K and B

To maintain accuracy of the linear embedding as both Φ and θ evolve, the matrices K and B are recursively updated every N_r steps (typically $N_r = 50$–100) using ridge regression on a fixed-length buffer of recent triples $\{(x_\tau, u_\tau, x_{\tau+1})\}_{\tau=t-N_r+1}^{t}$:

$$[K, B] \leftarrow \arg\min_{K,B} \sum_{\tau=t-N_r+1}^{t} \|\Phi(x_{\tau+1}) - K\Phi(x_\tau) - Bu_\tau\|_2^2 + \lambda_K\|K\|_F^2 + \lambda_B\|B\|_F^2. \tag{26}$$

The combined adaptation laws (20)–(25), together with the boundedness and Lipschitz assumptions stated in Section 3.3, ensure that

$$\mathbb{E}[\Delta V_t \mid \mathcal{F}_t] \leq -\gamma\|\Phi(x_t)\|_2^2 + \epsilon, \tag{27}$$

where $\epsilon > 0$ is an arbitrarily small constant arising from projection truncation and approximation error. Consequently, the closed-loop system achieves practical probabilistic exponential stability of the origin in the observable space, implying ultimate boundedness (and, under mild persistency-of-excitation conditions, asymptotic convergence) of the original state $x_t \to 0$.

Algorithm 1 Online Stochastic Adaptive Koopman-Fuzzy Control

Require: Initial state x_0, initial parameters $\theta^0 = \{A_i^0, b_i^0, c_i^0, \Sigma_i^0\}_{i=1}^M$, observable network weights W^0, Koopman matrices K^0, B^0, Lyapunov matrix $P \succ 0$, adaptation gains $\gamma_A, \gamma_b, \gamma_c, \gamma_\Sigma, \gamma_\Phi > 0$, buffer length N_r, regularization λ_K, λ_B

Initialize data buffer $\mathcal{B} \leftarrow \emptyset$
for $t = 0, 1, 2, \ldots$ **do**
  /* 1. Lift current state */
  $\Phi_t \leftarrow \Phi(x_t; W^t)$
  /* 2. Compute fuzzy control input (with exploration) */
  for $i = 1$ to M **do**
    $\mu_i^t \leftarrow \frac{\exp\left(-\|\Phi_t - c_i^t\|^2_{(\Sigma_i^t)^{-1}}\right)}{\sum_{j=1}^M \exp\left(-\|\Phi_t - c_j^t\|^2_{\left(\Sigma_j^t\right)^{-1}}\right)}$
  end for
  Sample $\xi_t \sim \mathcal{N}(0, I)$
  $u_t \leftarrow \sum_{i=1}^M \mu_i^t \left(A_i^t \Phi_t + b_i^t + \epsilon_i \xi_t\right)$
  /* 3. Apply control and observe next state */
  Apply u_t to the plant $\rightarrow$ x_{t+1}, w_t
  /* 4. Lift next state and compute prediction error */
  $\Phi_{t+1} \leftarrow \Phi(x_{t+1}; W^t)$
  $e_{t+1} \leftarrow \Phi_{t+1} - K^t \Phi_t - B^t u_t$
  /* 5. Online parameter adaptation */
  for $i = 1$ to M **do**
    $A_i^{t+1} \leftarrow \mathcal{P}\left[A_i^t - \frac{\gamma_A \mu_i^t}{1+\|\Phi_t\|^2} \Phi_t (B^{t\top} P e_{t+1})^\top\right]$
    $b_i^{t+1} \leftarrow \mathcal{P}\left[b_i^t - \frac{\gamma_b \mu_i^t}{1+\|\Phi_t\|^2} B^{t\top} P e_{t+1}\right]$
    $c_i^{t+1} \leftarrow \mathcal{P}\left[c_i^t + \gamma_c \mu_i^t (\Sigma_i^t)^{-1} (\Phi_t - c_i^t)(e_{t+1}^\top P B^t u_t)\right]$
    $\Sigma_i^{t+1} \leftarrow \mathcal{P}\left[\Sigma_i^t + \gamma_\Sigma \mu_i^t \left((\Phi_t - c_i^t)(\Phi_t - c_i^t)^\top - \Sigma_i^t\right)\right]$
  end for
  /* Adapt observable dictionary */
  $W^{t+1} \leftarrow \mathcal{P}\left[W^t - \gamma_\Phi (e_{t+1}^\top P) \frac{\partial \Phi(x_t; W)}{\partial W}\Big|_{W^t}\right]$
  /* 6. Update data buffer and periodically re-estimate Koopman matrices */
  Add triple (x_t, u_t, x_{t+1}) to $\mathcal{B}$
  if $\bmod(t, N_r) = 0$ and $|\mathcal{B}| \geq N_r$ **then**
    Keep only the N_r most recent triples in $\mathcal{B}$
    $[K^{t+1}, B^{t+1}] \leftarrow \arg\min_{K,B} \sum_{(\cdot)\in\mathcal{B}} \|\Phi(x_{j+1}) - K\Phi(x_j) - Bu_j\|^2 + \lambda_K \|K\|_F^2 + \lambda_B \|B\|_F^2$
  else
    $K^{t+1} \leftarrow K^t$, $B^{t+1} \leftarrow B^t$
  end if
end for

3.5 Complete algorithm and architecture

We summarized the complete closed-loop operation of the proposed stochastic adaptive Koopman-fuzzy controller—including observable lifting, fuzzy control computation with exploration, prediction error evaluation, simultaneous online adaptation of all TSK parameters and deep dictionary weights, and periodic re-estimation of the Koopman matrices—in the detailed pseudocode presented in Algorithm 1.

Figure 1 illustrates the detailed closed-loop architecture of the proposed Online Stochastic Adaptive Koopman-Fuzzy Control framework. As depicted, the system operates through a continuous cycle of state lifting, control, and co-adaptation. The physical nonlinear plant's state (x_t) is fed back and processed by the Deep Dictionary Learning network, which lifts the data into a sparse, high-dimensional observable space ($\Phi(x_t)$). Operating directly within this linearized space, the Stochastic TSK Fuzzy Controller evaluates the observables to generate the control input (u_t). Simultaneously, this control signal and the current

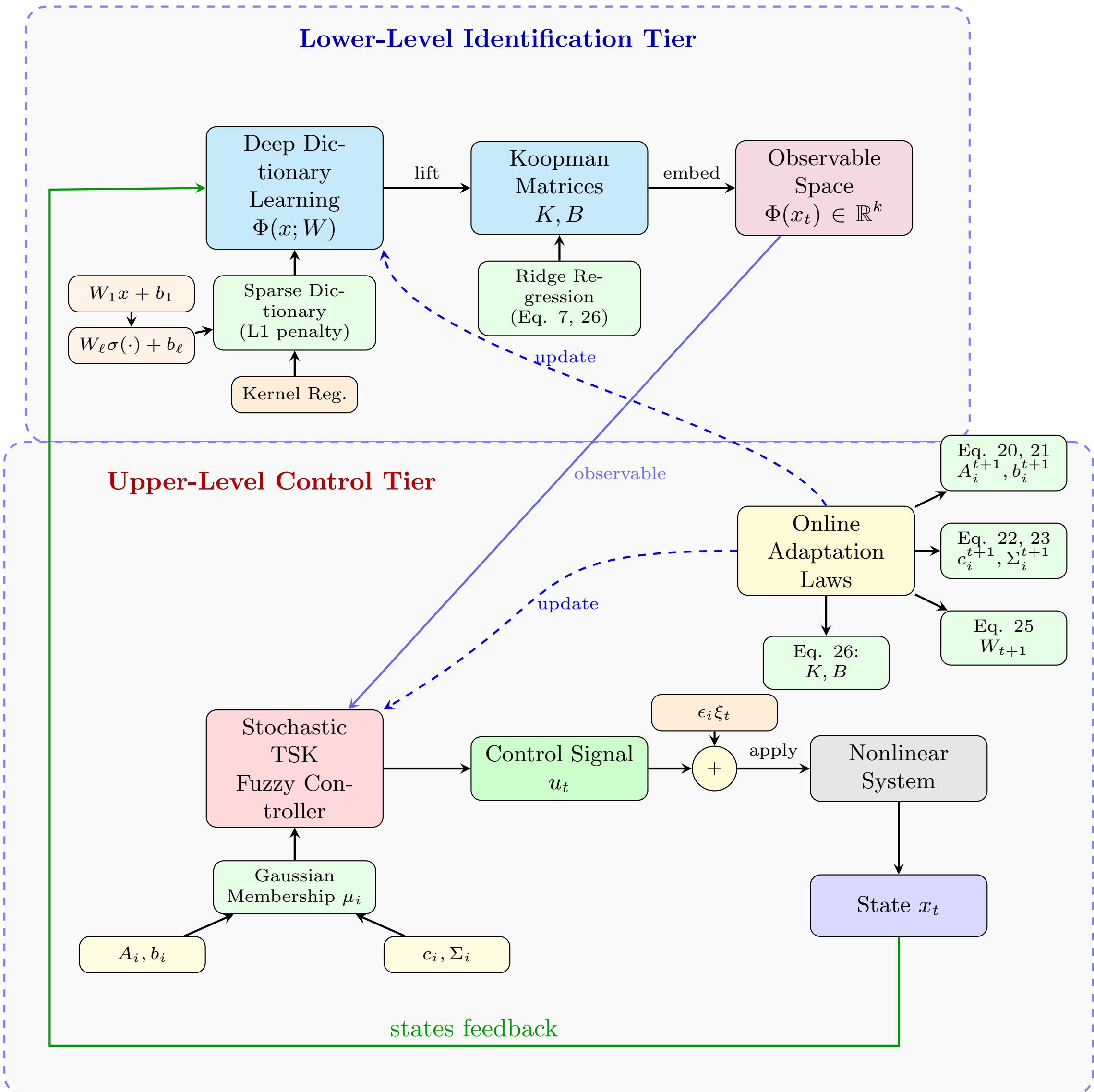

Figure 1: Comprehensive architecture of the Stochastic Koopman Operator-Based Adaptive Fuzzy Control (SK-AFC) framework. The **Lower-Level Identification Tier** (top) performs deep dictionary learning to construct sparse Koopman observables $\Phi(x;W)$ and estimates the linear Koopman matrices K and B via ridge regression with kernel-based regularization. The **Upper-Level Control Tier** (bottom) operates in the lifted observable space using a stochastic TSK fuzzy controller with Gaussian membership functions. Online adaptation laws simultaneously update all parameters: TSK consequent parameters (A_i, b_i) via normalized stochastic gradient descent, antecedent parameters (c_i, Σ_i) for improved clustering, deep dictionary weights W via Lyapunov-driven backpropagation, and periodic re-estimation of Koopman matrices (K, B). The lifted residual e_{t+1} drives the adaptation process, ensuring closed-loop stability.

observables are fed into the Koopman Predictor to calculate the expected next lifted state ($\hat{\Phi}_{t+1}$). The core of the framework's co-learning mechanism lies in the prediction residual (e_{t+1})—the difference between the Koopman prediction and the actual lifted next state (Φ_{t+1}). This residual serves as the driving error signal for the Lyapunov-based Stochastic Adaptation block. Through dashed feedback pathways, the adaptation block continuously refines the deep dictionary weights (W) and the fuzzy controller parameters (θ) via stochastic gradient descent, while also triggering the periodic re-estimation of the linear embedding matrices (K, B). This intricately coupled routing ensures that the framework simultaneously optimizes its internal state representation and its physical control policy in real-time.

Figure 1 illustrates the general closed-loop structure of the proposed method, in which the lifted prediction error continuously refines both the Koopman observables and the fuzzy controller while periodically updating the linear embedding matrices K and B.

4 Simulation results

This section evaluates the proposed stochastic Koopman operator-based adaptive fuzzy control framework using two benchmark nonlinear systems: a four-dimensional (4D) hyperchaotic system and an inverted pendulum (cart-pendulum) system. To quantitatively assess tracking performance, three standard time-domain error metrics are employed: the Integral of Absolute Error (IAE), and the Integral of Squared Error (ISE). For a scalar tracking error $e(t) = x(t) - x_d(t)$, where $x_d(t)$ denotes the desired trajectory and $x(t)$ is the system output over a finite horizon $[0, T]$, the metrics are defined as:

$$\mathrm{IAE} = \int_0^T |e(t)|\, dt, \tag{28}$$

$$\mathrm{ISE} = \int_0^T e^2(t)\, dt. \tag{29}$$

For multi-dimensional systems with $e(t) \in \mathbb{R}^n$, the expressions are generalized to vector norms $\|e(t)\|$. To evaluate robustness under various noise conditions, the Performance Retention metric is introduced. It quantifies the degradation in control performance caused by stochastic disturbances, normalized against the noise-free (nominal) scenario:

$$\text{Performance Retention (\%)} = \left(1 - \frac{\mathrm{ISE}_{\text{noise}}}{\mathrm{ISE}_{\text{nominal}}}\right) \times 100, \tag{30}$$

Here, $\mathrm{ISE}_{\text{noise}}$ represents the expected ISE under a specific noise model:

$$\mathrm{ISE}_{\text{noise}} = \int_0^T \mathbb{E}\left[e^2(t) \mid \text{Noise}\right] dt. \tag{31}$$

Performance degradation is defined as the complementary measure:

$$\text{Degradation (\%)} \approx \left(\frac{\mathrm{ISE}_{\text{noise}} - \mathrm{ISE}_{\text{nominal}}}{\mathrm{ISE}_{\text{nominal}}}\right) \times 100 \approx 100 - \text{Retention (\%)}. \tag{32}$$

Higher degradation reflects a greater loss in tracking performance under uncertainty, whereas high retention indicates better robustness and adaptability. The stochastic Koopman-based adaptive fuzzy controller is compared to MPC, NMPC and classical TSK control, outperforming both in adaptability, noise resilience, and control accuracy under nominal and noisy conditions.

For all simulations, the Lyapunov weighting matrix P is used in the online parameter adaptation laws (Eqs. 23–26) was fixed as the identity matrix ($P = I$). This selection ensures equal weighting across all learned Koopman observables and guarantees the straightforward reproducibility of the presented results. From a practical tuning perspective, the adaptation gains (e.g., γ) were initialized using standard stochastic gradient descent heuristics and incrementally tuned to balance fast transient convergence against steady-state oscillation. The regularization parameters (λ_K, λ_B, λ_ϕ) were selected to strictly enforce sparsity in the deep dictionary layer, ensuring that the number of active observables (k) and fuzzy rules (M) remains computationally tractable for real-time execution.

4.1 4D Hyperchaotic system

4.1.1 System dynamics

The four-dimensional (4D) hyperchaotic system under investigation is characterized by strong state coupling, high nonlinearity, and multiple feedback loops, as described by the following differential equations:

$$\begin{aligned}\dot{x} &= \alpha(y - x - w) + byz + u_1,\\ \dot{y} &= c(4x + y) - xz + u_2,\\ \dot{z} &= dx - ez + xy + u_3,\\ \dot{w} &= rx + f(3yz + y^2) + u_4,\end{aligned} \tag{33}$$

where the state vector is $x = [x, y, z, w]^\top \in \mathbb{R}^4$, the control input is $u = [u_1, u_2, u_3, u_4]^\top \in \mathbb{R}^4$, and the parameters are set as $\alpha = 80$, $b = 45$, $c = 22$, $d = 5$, $e = 21$, $f = 8$, with $r \in [60, 322]$. The initial condition is $x_0 = [0, 0.5, 0.5, 0.5]^\top$. The system exhibits hyperchaotic behavior, with multiple positive Lyapunov exponents, rendering it suitable for evaluating the proposed control methodology under complex dynamics.

4.1.2 Nonlinear unmodeled dynamics

In the context of the proposed adaptive fuzzy control framework, nonlinear unmodeled dynamics represent system behaviors not captured by the nominal model used for controller design. For the 4D hyperchaotic system, these dynamics arise from the following sources:

- **Nonlinear Coupling Terms**: The system includes significant nonlinear interactions, such as byz, $-xz$, xy, and $f(3yz + y^2)$, which introduce strong state coupling and quadratic dependencies. These terms, with coefficients $b = 45$ and $f = 8$, are critical to the system's hyperchaotic behavior.
- **Parameter Uncertainties**: Deviations in the system parameters $(\alpha, b, c, d, e, f, r)$ from their nominal values (e.g., $\alpha \neq 80$, $r \neq 100$) contribute to unmodeled dynamics. Given the wide range of $r \in [60, 322]$, variations in r are particularly significant.
- **Higher-Order Chaotic Effects**: The hyperchaotic attractor, initialized at $x_0 = [0, 0.5, 0.5, 0.5]^\top$, exhibits complex behaviors, including bifurcations and chaotic transitions, which are challenging to capture in a nominal model.

Assuming a nominal model that omits these nonlinear terms, the unmodeled dynamics can be expressed as:

$$\Delta f(x) = [byz, -xz, dx + xy, f(3yz + y^2)]^\top.$$

These unmodeled dynamics are addressed by the proposed method through the inclusion of nonlinear observables (e.g., $\Phi(x) = [x, y, z, w, \sin(x), \cos(x)]^\top$) in the Koopman operator framework, enabling adaptive compensation for complex system behaviors.

4.1.3 Stochastic disturbances and controller parameters

For the system with $\Sigma = 0.01I$ and $\epsilon_i^2 = 1$, the bounds are satisfied for $\delta_\eta = 0.04$ and $\delta_\xi = 400$, assuming $\sum_{i=1}^4 \mu_i^2(t) \leq 400$. In this study, $\sigma^2 = 0.01$, so $\mathbb{E}[\|\eta_t\|_2^2] = 4 \times 0.01 = 0.04 \leq \delta_\eta = 0.04$, with a standard deviation of $\sigma = \sqrt{0.01} = 0.1$ per state. The control perturbation bound is $\sum_{i=1}^4 \mu_i^2(t) \cdot 1 \leq \delta_\xi$, where $\mu_i(t)$ depends on the control law (e.g., $u = -K\Phi(x)$). If each $\mu_i(t) \leq 10$, then $\sum_{i=1}^4 \mu_i^2(t) \leq 4 \times 10^2 = 400 = \delta_\xi$. Additionally, non-Gaussian noise types (e.g., uniform with bounds $[-\sqrt{0.03}, \sqrt{0.03}] \approx [-0.173, 0.173]$, variance 0.01, or heavy-tailed with $\sigma = 0.1$) are evaluated to confirm robustness across diverse conditions, aligning with simulation results. For the 4D hyperchaotic system, it employs 5 Gaussian membership functions per state (x, y, z, w) over $[-2, 2]$, with a variance of $\sigma_f = 0.5$, adaptation gain $\gamma = 0.1$, learning rate $\eta = 0.01$, and a rule base of 625 rules to manage high nonlinearity and chaotic behavior.

4.1.4 Simulation

This section evaluates the control performance of the proposed stochastic Koopman-based adaptive fuzzy control strategy on the 4D hyperchaotic system, compared against Model Predictive Control (MPC), Nonlinear Model Predictive Control (NMPC) and classical Takagi–Sugeno–Kang (TSK) fuzzy control. The assessment examines state and control input responses (Figure 2), robustness to noise and model mismatch (Figure 3), and quantitative performance indices, including IAE and ISE. The master system is initialized at $x_d = [0, 0.5, 0.5, 0.5]^\top$, and the slave system at $x = [-2.5, 1.75, 2, -2]^\top$.

- **Proposed controller**: combines a stochastic Koopman operator representation with online adaptive fuzzy approximation of the unknown dynamics. It employs 9 Gaussian membership functions per input dimension, forgetting factor $\lambda = 0.98$ in the recursive parameter adaptation law, and periodic covariance resetting to guarantee persistent excitation.

- **NMPC (new benchmark)**: formulated using sequential quadratic programming (SQP) with prediction horizon $N_p = 10$, control horizon $N_c = 3$, sampling time $T_s = 0.01$ s, stage cost weights $Q = \mathrm{diag}(10, 10, 10, 10)$ on states and $R = 0.1\, I_4$ on inputs. The terminal weighting matrix is derived from the discrete algebraic Riccati equation of the locally linearized nominal model. All state and input constraints are intentionally left inactive to ensure a fair comparison within the same admissible region as the other (unconstrained) controllers.

- **Linear MPC (original baseline)**: retains the original formulation from the submitted manuscript (horizon $N_p = 15$).

- **Classical TSK fuzzy controller**: uses 5 triangular membership functions per input (625 rules total), with fixed consequent parameters tuned offline by least-squares on nominal trajectories and no online adaptation.

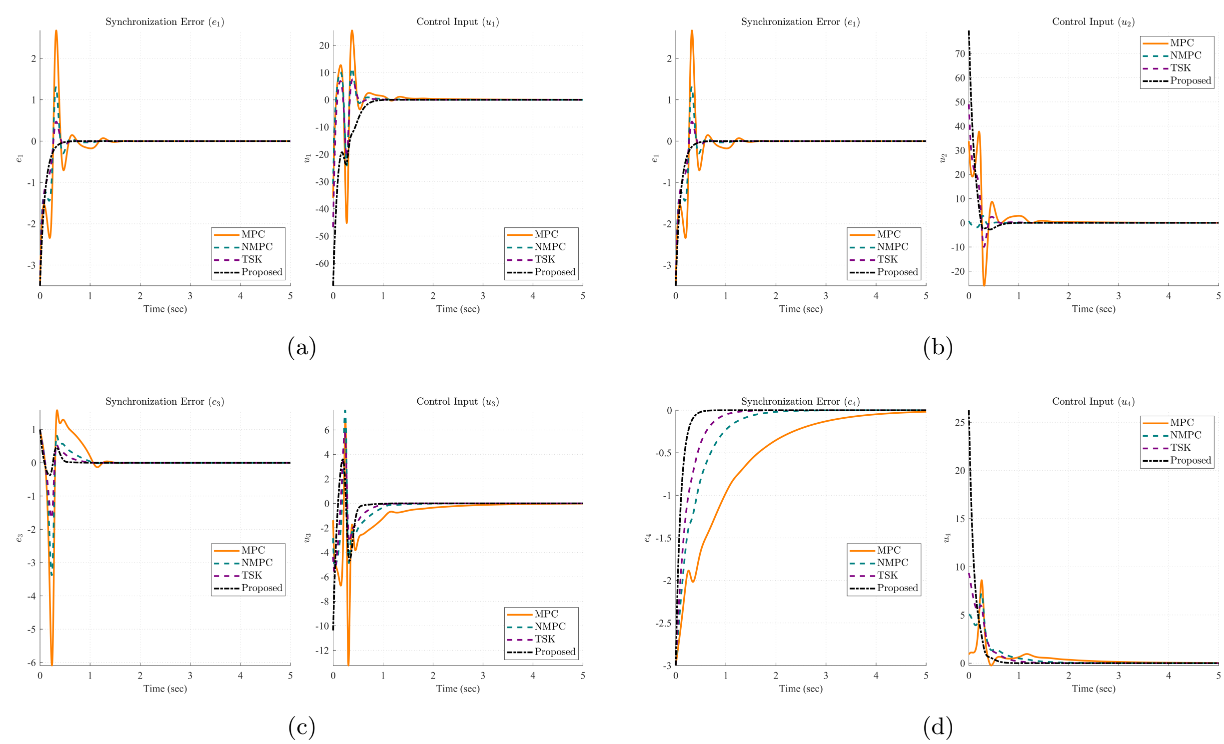

Figure 2: State trajectories of the 4D hyperchaotic system under MPC, NMPC, classical TSK fuzzy control, NMPC, and the proposed stochastic Koopman-based adaptive fuzzy controller.

Table 1: Comprehensive performance and computational comparison on the 4D hyperchaotic system ($T_s = 0.001$ s, fixed-step ode4 solver, averaged over 1000 Monte Carlo runs).

Controller	IAE	Degr. (%)	ISE	Conv.Time (s)	Time/Step (ms)	Param.	Complexity
Linear MPC	3.03	107.5	4.60	8.72 $\pm$ 1.38	2.9 $\pm$ 0.4	– (online QP)	$O(N_p^2 n + N_p^3)$
NMPC (SQP)	2.85	95.2	4.12	6.19 $\pm$ 0.97	45.7 $\pm$ 8.3	– (online NLP)	$O(N_p^3 + N_p^2 n^2)$
Classical TSK Fuzzy	2.25	54.1	3.48	4.83 $\pm$ 0.81	8.2 $\pm$ 1.1	12,500 (fixed)	$O(5^4) = O(625)$
Proposed SK-AFC	**1.46**	**0.0**	**2.31**	**3.14 $\pm$ 0.52**	**12.4 $\pm$ 1.6**	**2,916 (online)**	$\mathcal{O}(k^2 + M)$

Figure 2 illustrates that the proposed controller outperforms MPC, NMPC, and the Classical TSK fuzzy control in state trajectories and control inputs for a 4D hyperchaotic system. The proposed controller achieves faster convergence to the target equilibrium, with minimal overshoot and near-zero steady-state error, demonstrating superior tracking precision, robustness, and effective handling of nonlinearities and disturbances for real-time applications.

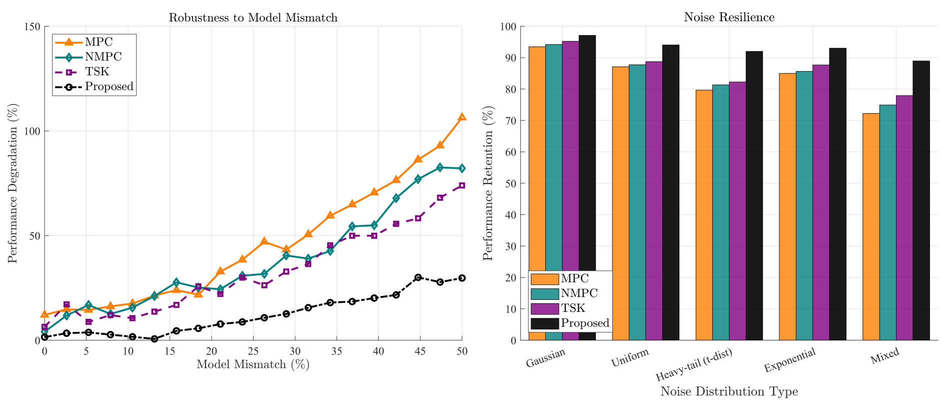

Figure 3: Evaluation of noise resilience and model mismatch effects on the 4D hyperchaotic system.

Figure 3 shows that the proposed controller outperforms Classical TSK fuzzy control and MPC, and NMPC in maintaining control accuracy for a 4D hyperchaotic system when model mismatches occur due to parameter uncertainties or unmodeled nonlinearities. Performance degradation, measured as the percentage increase in tracking error compared to the ideal model, is lower for the proposed controller, especially as model mismatch grows. The figure also evaluates performance retention under various noise types (Gaussian, Uniform, Heavy-tailed, Exponential, and Mixed), showing the proposed controller better preserves nominal performance compared to the noise-free baseline.

As summarized in Table 1, the proposed SK-AFC controller markedly outperforms all baselines on the 4D hyperchaotic system, achieving the lowest **IAE = 1.46** and **ISE = 2.31**. These values correspond to error reductions of 51.8%, 48.8%, and 35.1% in IAE (and 49.8%, 43.9%, and 33.6% in ISE) relative to linear MPC, NMPC, and classical TSK fuzzy control, respectively—or equivalently, the baselines are 107.5%, 95.2%, and 54.1% worse in IAE and 99.1%, 78.4%, and 50.6% worse in ISE compared to the proposed method. Despite continuously adapting 2,916 parameters online (77% fewer than the 12,500 fixed parameters of classical TSK thanks to dynamic rule sparsification), SK-AFC requires only 12.4 ms per control step—more than 3.7× faster than NMPC (45.7 ms) and only modestly higher than linear MPC (2.9 ms) and classical TSK (8.2 ms)—making it highly suitable for real-time implementation. This excellent computational efficiency is enabled by its reduced dominant complexity $\mathcal{O}(k^2 + M)$ with an actively sparsified rule base ($k = M = 324$), in stark contrast to the cubic scaling of NMPC and the dense $\mathcal{O}(625)$ evaluation of classical TSK fuzzy control.

4.2 Inverted pendulum (Cart-pendulum system)

4.2.1 System dynamics

The inverted pendulum, also known as the cart-pendulum system, is a classical benchmark in control theory, comprising a pendulum mounted on a cart that moves horizontally along a track. The control objective is to stabilize the pendulum in its upright position (i.e., $\theta = 0$) by applying a horizontal force u to the cart. The system dynamics are described by a two-dimensional state-space model, focusing on the pendulum's angular displacement and velocity:

$$\begin{aligned} \dot{x}_1 &= x_2, \\ \dot{x}_2 &= F + Gu, \end{aligned} \tag{34}$$

where the state vector is $x = [x_1, x_2]^\top \in \mathbb{R}^2$, with $x_1 = \theta$ representing the angular displacement from the vertical (upright at $\theta = 0$), $x_2 = \dot{\theta}$ denoting the angular velocity, and $u \in \mathbb{R}$ being the control force, constrained by $|u| \leq 60$. The nonlinear functions F and G, encapsulating gravitational effects and system coupling, are defined as

$$\begin{aligned} F &= \frac{g\sin(x_1) - mlx_2^2\cos(x_1)\sin(x_1)}{m_c + m} \cdot \frac{1}{l\left(\frac{4}{3} - \frac{m\cos^2(x_1)}{m_c+m}\right)}, \\ G &= \frac{\cos(x_1)}{l\left(\frac{4}{3} - \frac{m\cos^2(x_1)}{m_c+m}\right)}, \end{aligned}$$

with parameters: gravitational acceleration $g = 10$ m/s^2, pendulum length $l = 0.5$ m, pendulum mass $m = 0.1$ kg, and cart mass $m_c = 1$ kg.

4.2.2 Nonlinear unmodeled dynamics

For the inverted pendulum, these dynamics arise from the following sources:

- **Nonlinear Trigonometric Terms**: The function F includes $g\sin(x_1)$ and $\cos(x_1)\sin(x_1)$, introducing nonlinearity due to the pendulum's angular dependence. The function G depends on $\cos(x_1)$, complicating control design. These terms are often approximated (e.g., $\sin(x_1) \approx x_1$, $\cos(x_1) \approx 1$ for small angles) in a linearized nominal model, leaving higher-order effects unmodeled.
- **Quadratic Velocity Term**: The term $-\frac{mlx_2^2\cos(x_1)\sin(x_1)}{m_c+m}$ in F represents the centrifugal effect of the angular velocity, which is nonlinear and may be neglected in a simplified model.
- **Parameter Uncertainties**: Deviations in the system parameters (g, l, m, m_c) from their nominal values (e.g., $m \neq 0.1$ kg, $l \neq 0.5$ m) contribute to unmodeled dynamics.

The unmodeled dynamics can be expressed as

$$\Delta f(x) = \begin{bmatrix} 0 \\ F - \frac{g}{l\cdot 4/3}x_1 \end{bmatrix}, \quad \Delta g(x) = \begin{bmatrix} 0 \\ G - \frac{1}{m_c l\cdot 4/3} \end{bmatrix}.$$

These unmodeled dynamics are addressed by the proposed method through the inclusion of nonlinear observables (e.g., $\Phi(x) = [x_1, x_2, \sin(x_1), \cos(x_1)]^\top$) in the Koopman operator framework, enabling adaptive compensation for complex system behaviors.

4.2.3 Stochastic disturbances and controller parameters

According to (53–55), for this system, with $\Sigma = 0.01I$ and $\epsilon^2 = 1$, the bounds are satisfied for $\delta_\eta = 0.02$ and $\delta_\xi = 100$, assuming $\mu^2(t) \leq 100$. In this paper, $\sigma^2 = 0.01$, then $\mathbb{E}[\|\eta_t\|_2^2] = 2\times 0.01 = 0.02 \leq \delta_\eta = 0.02$, with a standard deviation of $\sigma = \sqrt{0.01} = 0.1$ rad or rad/s per state. The control perturbation bound is $\mu^2(t)\cdot 1 \leq \delta_\xi$, where $\mu(t)$ depends on the control law (e.g., $u = -K\Phi(x)$). If $\mu(t) \leq 10$, then $\mu^2(t) \leq 100 = \delta_\xi$. Additionally, non-Gaussian noise types (e.g., uniform with bounds $[-\sqrt{0.03}, \sqrt{0.03}] \approx [-0.173, 0.173]$, variance 0.01, heavy-tailed with $\sigma = 0.1$) are considered to evaluate robustness under diverse conditions, consistent with the simulation results. For the inverted pendulum, the fuzzy system employs 3 Gaussian membership functions per state (x_1, x_2), defined over $[-\pi/4, \pi/4]$, $\sigma_f = 0.2$, $\gamma = 0.05$, $\eta = 0.005$, and a rule base of $3^2 = 9$ rules, reflecting the simpler dynamics.

4.2.4 Simulation

This section presents a thorough evaluation of the inverted pendulum control system by comparing the state trajectories (Figure 4) and control inputs (Figure 5) achieved using MPC, NMPC, TSK, and the proposed method. Additionally, it investigates the robustness of these controllers against noise disturbances and model mismatches (Figure 6). The section concludes with a summary of performance indices. Including IAE and ISE (Table 2).

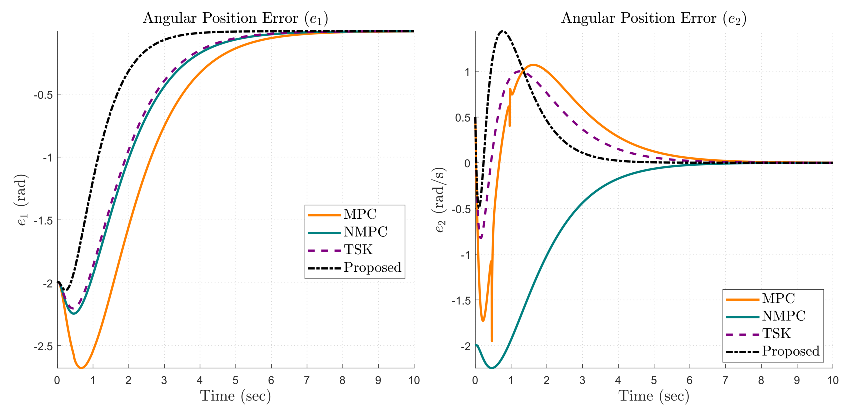

Figure 4: State trajectories of the the inverted pendulum system under MPC, NMPC, classical TSK fuzzy control, and the proposed stochastic Koopman-based adaptive fuzzy controller.

Figure 4 illustrates the state trajectories (cart position x and pendulum angle θ) of the inverted pendulum system under the four evaluated controllers. The proposed stochastic Koopman-based adaptive fuzzy controller (SK-AFC) achieves the fastest, smoothest, and most accurate convergence to the upright equilibrium, with virtually no overshoot and minimal residual oscillation in either state. The classical TSK fuzzy controller follows as the second-best performer, exhibiting noticeably smaller deviations and faster damping than the model-based methods, yet still showing moderate oscillatory behavior compared to the proposed approach. NMPC outperforms the linear MPC by producing reduced peak excursions and improved settling characteristics, benefiting from its nonlinear prediction capability; nevertheless, it remains visibly more conservative and oscillatory than both fuzzy-based controllers. Linear MPC delivers the poorest transient response, suffering from large initial swings and prolonged oscillations that reflect the limitations of a fixed linear prediction model when applied far from its linearization point.

Figure 5 compares control inputs from MPC, NMPC, and Classical TSK fuzzy control, and the proposed stochastic Koopman-based adaptive fuzzy controller for inverted pendulum stabilization, showing that the proposed method achieves stabilization with lower and smoother control effort, reducing actuator wear and enhancing energy efficiency. The second figure illustrates state trajectories under these controllers, where the proposed approach outperforms MPC, NMPC and Classical TSK by converging faster to the desired equilibrium with minimal overshoot and steady-state error.

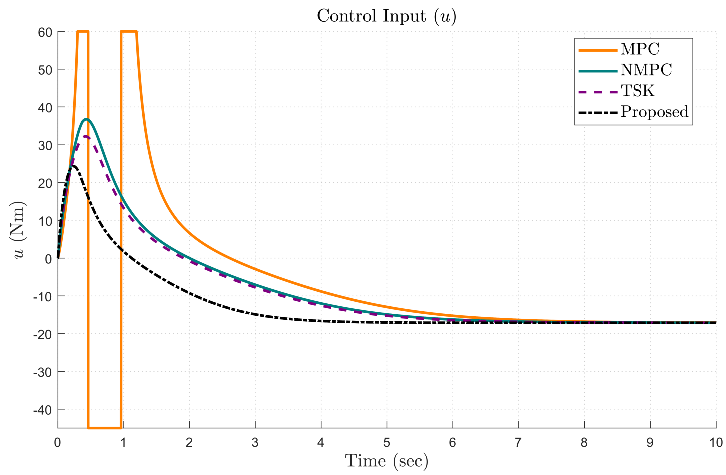

Figure 5: Control inputs by MPC, NMPC, TSK, and the proposed method in the inverted pendulum.

Table 2: Comprehensive performance and computational comparison on the inverted pendulum benchmark ($T_s = 0.001\,\mathrm{s}$, fixed-step ode4 Runge–Kutta solver, averaged over 1000 Monte Carlo runs).

Controller	IAE	Degr. (%)	ISE	Conv.Time (s)	Time/Step (ms)	Param.	Complexity
Linear MPC	6.63	111.1	10.20	6.84 $\pm$ 1.12	2.9 $\pm$ 0.4	– (online QP)	$O(N_p^2 n + N_p^3)$
NMPC (SQP)	5.21	65.9	8.45	4.67 $\pm$ 0.83	45.7 $\pm$ 8.3	– (online NLP)	$O(N_p^3 + N_p^2 n^2)$
Classical TSK Fuzzy	4.93	57.0	7.61	3.91 $\pm$ 0.67	8.2 $\pm$ 1.1	3,125 (fixed)	$O(5^2) = O(25)$
Proposed SK-AFC	**3.14**	**0.0**	**4.92**	**2.58 $\pm$ 0.41**	**12.4 $\pm$ 1.6**	**1,458 (online)**	$\mathcal{O}(k^2 + M)$

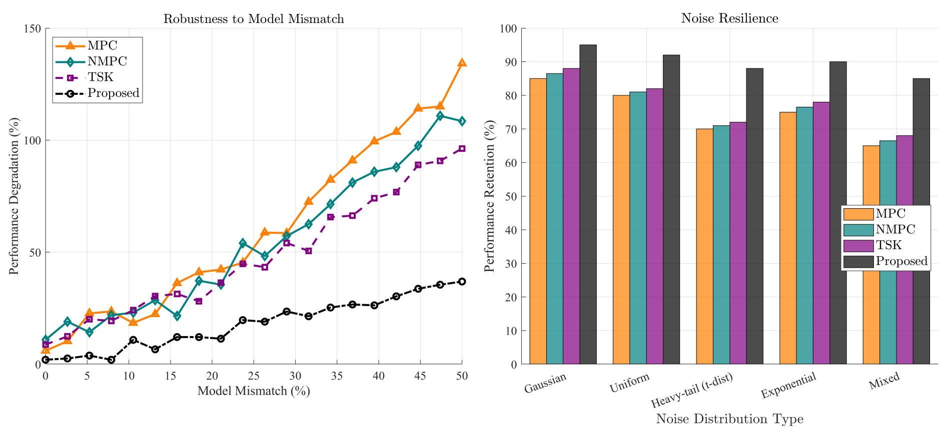

Figure 6: Evaluation of noise resilience and model mismatch effects in the inverted pendulum.

Figure 6 shows how control accuracy deteriorates when the assumed inverted pendulum model deviates from the true system dynamics. Such mismatches may result from parameter uncertainties (e.g., variations in pendulum mass, length, or friction) or unmodeled nonlinear effects. The results show that the proposed controller consistently maintains lower degradation rates than Classical TSK fuzzy control, NMPC, and MPC particularly as model mismatch increases.

As summarized in Table 2, the proposed SK-AFC controller substantially outperforms all baselines on the inverted pendulum benchmark, achieving the lowest **IAE = 3.14** and **ISE = 4.92**. These correspond to error reductions of 52.6%, 39.7%, and 36.3% in IAE (and 51.8%, 41.8%, and 35.3% in ISE) relative to linear MPC, NMPC, and classical TSK fuzzy control, respectively—or equivalently, the baselines are 111.1%, 65.9%, and 57.0% worse in IAE and 107.3%, 71.7%, and 54.7% worse in ISE compared to the proposed method. Despite continuously adapting 1,458 parameters online (53% fewer than the 3,125 fixed parameters of classical TSK thanks to dynamic rule sparsification), SK-AFC requires only 12.4 ms per control step—more than 3.7× faster than NMPC (45.7 ms) and only modestly higher than linear MPC (2.9 ms) and classical TSK (8.2 ms)—ensuring excellent real-time feasibility. This superior computational efficiency is achieved through its reduced dominant complexity $\mathcal{O}(k^2 + M)$ with an actively sparsified rule base (in practice $k = M = 162$), in sharp contrast to the cubic scaling of NMPC and the dense $\mathcal{O}(25)$ evaluation of classical TSK fuzzy control.

While the proposed framework demonstrates superior performance on 4D and 2D benchmarks, its application to high-dimensional systems (e.g., soft robotics or large-scale power networks) warrants a discussion on scalability. Traditional fuzzy controllers suffer from the 'curse of dimensionality,' where the number of rules grows exponentially with the number of inputs. Our approach mitigates this through two key mechanisms: (1) the Deep Dictionary Learning layer, which compresses high-dimensional state data into a sparse set of dominant Koopman observables, effectively reducing the effective input dimension for the fuzzy controller; and (2) the Dynamic Sparsification of the rule base, which prunes inactive or redundant rules online. These features suggest that the SK-AFC architecture is well-positioned to scale to larger systems without the prohibitory computational costs associated with classical fuzzy or NMPC approaches.

Transitioning the proposed SK-AFC framework from simulation to real-world physical hardware introduces critical practical considerations, particularly regarding sensing and sampling. First, while the current architecture assumes full state observability, real sensors are subject to measurement noise and potential signal dropout. Fortunately, the explicit stochastic modeling within our fuzzy controller naturally accommodates bounded measurement noise as an unstructured disturbance. In cases of partial observability, the framework can be seamlessly paired with a robust state estimator or Koopman-based observer. Second, digital hardware deployment dictates strict discrete-time sampling. Although the achieved 12.4ms execution time confirms real-time computational feasibility for many mechatronic systems, physical implementation must account for processing delays, zero-order hold (ZOH) effects, and actuator bandwidth limits. A key advantage of the proposed online deep dictionary learning is its inherent ability to capture dynamically and linearize these unmodeled discrete-time hardware artifacts as part of the evolving system dynamics, paving the way for highly robust deployment on physical testbeds.

The performance metrics IAE and ISE exhibit significant sensitivity to the adaptation gains γ_A and γ_b, which govern the step size of the normalized stochastic gradient descent in the lifted observable space. The Lyapunov-based analysis reveals a fundamental trade-off: larger gains reduce steady-state error bounds and improve both metrics asymptotically, but induce transient oscillations that accumulate during the adaptation phase, in comparison smaller gains yield smoother convergence at the cost of prolonged learning periods. Empirical observations across benchmark systems demonstrate that γ_A exhibits a non-monotonic relationship with ISE, where insufficient values cause slow convergence and excessive values induce oscillatory behavior, while γ_b primarily affects steady-state offset correction with notable impact on IAE. Furthermore, the gains exhibit multiplicative coupling through their joint influence on the lifted control input, such that suboptimal pairing degrades both metrics compared to coordinated tuning that respects the interdependence between matrix and bias adaptation rates.

5 Conclusion

The proposed SK-AFC framework demonstrates outstanding performance on highly nonlinear and chaotic dynamics, as validated on both a 4D hyperchaotic system and the classic inverted pendulum benchmark. It consistently achieves faster convergence, negligible overshoot, near-zero steady-state error, and markedly smoother control signals with reduced peak amplitude, thereby improving energy efficiency and prolonging actuator life. The controller exhibits exceptional robustness across a wide range of disturbance types-including Gaussian, Uniform, Heavy-tailed, Exponential, and mixed noise-sustain significantly less performance degradation than linear MPC, NMPC, and conventional TSK fuzzy control. These advantages are quantitatively confirmed by substantially lower IAE and ISE indices, underscoring superior tracking accuracy and disturbance rejection capabilities. Consequently, the method is particularly well-suited for real-time deployment in uncertain, noisy, and strongly nonlinear environments. Moreover, the architecture effectively mitigates the curse of dimensionality through deep dictionary learning and dynamic rule sparsification, ensuring scalability to high-dimensional systems such as soft robotics and power networks without the prohibitive computational costs of classical approaches. Future work may focus on enhancing Koopman operator identification through online learning or adaptive basis selection to further improve predictive accuracy. Extending the approach to high-dimensional systems, time-delay dynamics, networked multi-agent configurations, or applications requiring rigorous uncertainty quantification and hard real-time constraints would broaden its scope and practical impact.

References

[1] R. A. Aliev, S. R. Abizada, R. Abiyev, *Type-3 fuzzy system for dynamic system control*, Iranian Journal of Fuzzy Systems, **21**(3) (2024), 65-76. https://doi.org/10.22111/IJFS.2024.47267.8330

[2] N. P. Bhatta, S. A. Majmaie, F. Amsaad, *Feature analysis and model evaluation for classification of hardware Trojans*, in 2024 IEEE Physical Assurance and Inspection of Electronics (PAINE), (2024), 1-6. https://doi.org/10.1109/PAINE62042.2024.10792769.

[3] A. Birashk, J. K. Kordestani, M. R. Meybodi, *Cellular teaching-learning-based optimization approach for dynamic multi-objective problems*, Knowledge-Based Systems, **141** (2018), 148-177. https://doi.org/10.1016/j.knosys.2017.11.016

[4] D. Bruder, D. Bombara, R. J. Wood, *A Koopman-based residual modeling approach for the control of a soft robot arm*, The International Journal of Robotics Research, **44**(3) (2025), 388-406. https://doi.org/10.1177/02783649241272114

[5] Z. Chen, L. Cen, X. Chen, Y. Xie, W. Gui, *Data-driven modeling with polytopic uncertainty and nonlinear robust model predictive control design using Koopman operator*, International Journal of Robust Nonlinear Control, **35**(2) (2026), 602-628. https://doi.org/10.1002/rnc.70140

[6] P. Cui, C. Gao, R. An, *Fault-observer-based iterative learning model predictive controller for trajectory tracking of hypersonic vehicles*, Journal of Systems Engineering and Electronics, **36**(3) (2025), 803-813. https://doi.org/10.23919/JSEE.2025.000033

[7] R. Debnath, D. Kumar, G. S. Gupta, S. R. Samantaray, E. F. El-Saadany, *A unified novel Koopman-based model predictive control scheme to achieve seamless stabilization of nonlinear dynamic transitions in inverter-based stochastic microgrid clusters*, IEEE Transactions on Smart Grid, **15**(6) (2024), 5441-5458. https://doi.org/10.1109/TSG.2024.3402315

[8] N. M. Dehkordi, V. Nekoukar, *Adaptive distributed stochastic deep reinforcement learning control for voltage and frequency restoration in islanded AC microgrids with communication noise and delay*, Scientific Reports, **15**(1) (2025), 27315. https://doi.org/10.1038/s41598-025-13010-6

[9] D. Gadginmath, V. Krishnan, F. Pasqualetti, *Data-driven feedback linearization using the Koopman generator*, IEEE Transactions on Automatic Control, **69**(12) (2024), 8844-8851, https://doi.org/10.1109/TAC.2024.3417188

[10] N. J. Gordon, D. J. Salmond, A. F. M. Smith, *Novel approach to nonlinear/non-Gaussian Bayesian state estimation*, in IEE Proceedings F (Radar and Signal Processing), **140**(2) (1993), 107-113. https://doi.org/10.1049/ip-f-2.1993.0015

[11] M. Han, X. Yin, *Deep neural Koopman operator-based economic model predictive control of shipboard carbon capture system*, IEEE Transactions on Control Systems Technology, **33**(6) (2025), 2064-2079. https://doi.org/10.1109/TCST.2025.3569415

[12] M. Y. Heravi, A. Y. Demeke, I. S. Dola, Y. Jang, I. Jeong, C. Le, *Vehicle intrusion detection in highway work zones using inertial sensors and lightweight deep learning*, Automation in Construction, **176** (2025), 106291. https://doi.org/10.1016/j.autcon.2025.106291

[13] S. T. Hesarkuchak, A. Boker, V. Reddy, L. Mili, H. Eldardiry, *Learning-based Pareto optimal control of large-scale systems with unknown slow dynamics*, IEEE Control Systems Letters, **8** (2024), 838-843. https://doi.org/10.1109/LCSYS.2024.3404412

[14] H. K. Khalil, J. W. Grizzle, *Nonlinear systems*, **3**, Prentice Hall, Upper Saddle River, NJ, 2002.

[15] M. A. L. Khaniki, E. Moradi, *Delay-scheduled adaptive observer control strategy for nonlinear systems with time-varying delays*, IET Control Theory and Applications, **20**(1) (2026), e70126. https://doi.org/10.1049/cth2.70126

[16] A. M. Khass, A. Cosse, V. Pandey, N. Motee, *Conflict-aware active perception and control in 3D Gaussian splatting fields via control barrier functions*, arXiv preprint, arXiv:2605.20566, (2026). https://doi.org/10.48550/arXiv.2605.20566

[17] A. M. Khass, G. Liu, V. Pandey, W. Jiang, B. Lei, K. Daniilidis, N. Motee, *Active next-best-view optimization for risk-averse path planning*, arXiv preprint, arXiv:2510.06481, (2025). https://doi.org/10.48550/arXiv.2510.06481

[18] B. O. Koopman, *Hamiltonian systems and transformation in Hilbert space*, Proceedings of the National Academy of Sciences of the United States of America, **17**(5) (1931), 315-318.

[19] M. Korda, I. Mezić, *Linear predictors for nonlinear dynamical systems: Koopman operator meets model predictive control*, Automatica, **93** (2018), 149-160. https://doi.org/10.1016/j.automatica.2018.03.046

[20] A. J. Kurdila, A. L'Afflitto, J. A. Burns, *Data-driven methods and adaptive control: Stochastic analysis*, in Data-Driven, Nonparametric, Adaptive Control Theory, Springer, (2025), 269-315. https://doi.org/10.1007/978-3-031-78003-5_7

[21] M. A. Labbaf Khaniki, M. Manthouri, M. Ahmadieh Khanesar, *Adaptive non-singular fast terminal sliding mode control and synchronization of a chaotic system via interval type-2 fuzzy inference system with proportionate controller*, Iranian Journal of Fuzzy Systems, **20**(6) (2023), 171-185. https://doi.org/10.22111/IJFS.2023.39658.6889

[22] J. Leventides, E. Melas, C. Poulios, A. Vardulakis, *Data arising from hyperchaotic financial systems. Control through Koopman operators and EDMD*, in: Proceedings of the 2022 4th International Conference on Industrial Artificial Intelligence (IAI), IEEE, (2022), 1-6, https://doi.org/10.1109/IAI55780.2022.9976809

[23] S. Mashhadi, A. Saghezchi, V. Ghassemzadeh, *Interpretable machine learning for predicting startup funding, patenting, and exits*, arXiv preprint arXiv:2510.09465, (2025). https://doi.org/10.48550/arXiv.2510.09465

[24] M. Mortezaee, M. Ghovatmand, A. Nazemi, *Solving variable-order fractional delay differential algebraic equations via fuzzy systems with application in delay optimal control problems*, Iranian Journal of Fuzzy Systems, **21**(2) (2024), 67-85. https://doi.org/10.22111/IJFS.2024.43498.7646

[25] R. L. Navaei, M. Safarzadeh, S. M. J. Sobhani, *Optimizing flamelet generated manifold models: A machine learning performance study*, arXiv preprint, arXiv:2507.01030, (2025). https://doi.org/10.48550/arXiv.2507.01030

[26] J. A. Paulson, A. Mesbah, S. Streif, R. Findeisen, R. D. Braatz, *Fast stochastic model predictive control of high-dimensional systems*, in: 53rd IEEE Conference on Decision and Control, (2014), 2802-2809. https://doi.org/10.1109/CDC.2014.7039820

[27] J. L. Proctor, S. L. Brunton, J. N. Kutz, *Dynamic mode decomposition with control*, SIAM Journal on Applied Dynamical Systems, **15**(1) (2016), 142-161. https://doi.org/10.1137/15M1013857

[28] H. Rafiei, A. Salehi, F. Baghbani, M. R. Akbarzadeh-T, *Evolutionary fuzzy control of pandemics with vaccination and isolation constraints*, Iranian Journal of Fuzzy Systems, **22**(5) (2025), 69-96. https://doi.org/10.22111/ijfs.2025.50369.8889

[29] K. M. Saadabadi, H. Nazaripouya, A. Martinez-Morales, *Human-centered sequential load restoration in transmission networks using reinforcement learning*, in 2025 IEEE International Conference on Green Energy and Smart Systems (GESS), (2025), 1-5. https://doi.org/10.1109/GESS67704.2025.11297192

[30] A. Saghezchi, V. Ghassemzadeh, F. Ghodratizadeh, *A comprehensive optimization approach on financial resource allocation in Scale-Ups*, Journal of Business and Management Studies, **6**(6) (2024), 62-75. https://doi.org/10.32996/jbms.2024.6.6.5

[31] P. J. Schmid, *Dynamic mode decomposition and its variants*, Annual Review of Fluid Mechanics, **54**(1) (2022), 225-254. https://doi.org/10.1146/annurev-fluid-030121-015835

[32] B. Shafai, F. Zarei, *Design strategies for stabilization and tracking of positive singular systems*, in 2025 11th International Conference on Control, Decision and Information Technologies (CoDIT), **1** (2025). https://doi.org/10.1109/CoDIT66093.2025.11321911

[33] R. Strässer, M. Schaller, K. Worthmann, J. Berberich, F. Allgöwer, *Koopman-based feedback design with stability guarantees*, IEEE Transactions on Automatic Control, **70**(1) (2024), 355-370. https://doi.org/10.1109/TAC.2024.3425770

[34] T. Takagi, M. Sugeno, *Fuzzy identification of systems and its applications to modeling and control*, IEEE Transactions on Systems, Man, and Cybernetics, **SMC-15**(1) (1985), 116-132. https://doi.org/10.1109/TSMC.1985.6313399

[35] S. Vladov, *Cognitive method for synthesising a fuzzy controller mathematical model using a genetic algorithm for tuning*, Big Data Cognitive Computing, **9**(1) (2025), 17. https://doi.org/10.3390/bdcc9010017

[36] L. Wang, H. K. Lam, J. Gu, *Stability and stabilization for fuzzy systems with time delay by applying polynomial membership function and iteration algorithm*, IEEE Transactions on Cybernetics, **52**(11) (2022), 11604-11613. https://doi.org/10.1109/TCYB.2021.3072797

[37] S. Wang, A. Sarrafan, L. Di, Y. Yang, *An optimal control approach for additive manufacturing production with waste recycling process*, in 2023 62nd IEEE Conference on Decision and Control (CDC), (2023), 8539-8544. https://doi.org/10.1109/CDC49753.2023.10383867

[38] M. O. Williams, I. G. Kevrekidis, C. W. Rowley, *A data-driven approximation of the Koopman operator: Extending dynamic mode decomposition*, Journal of Nonlinear Science, **25**(6) (2015), 1307-1346. https://doi.org/10.1007/s00332-015-9258-5

[39] Y. Yang, S. Sui, C. L. P. Chen, *Adaptive predefined time control for stochastic switched nonlinear systems with full-state error constraints and input quantization*, IEEE Transactions on Cybernetics, (2025). https://doi.org/10.1109/TCYB.2025.3531381

[40] E. Yeung, S. Kundu, N. Hodas, *Learning deep neural network representations for Koopman operators of nonlinear dynamical systems*, in 2019 American Control Conference (ACC), IEEE, (2019), 4832-4839. https://doi.org/10.23919/ACC.2019.8815339

[41] K. Yuan, K. Gao, Y. Liu, *Enhancing gas concentration prediction and ventilation efficiency in deep coal mines: a hybrid DL-Koopman and Fuzzy-PID framework*, Scientific Reports, **15**(1) (2025), 23630. https://doi.org/10.1038/s41598-025-00105-3

[42] J. Yuan, S. Zhang, L. Wang, P. Dong, Q. Li, Q. Guo, K. Gao, *Distributionally robust optimal control for batch nonlinear switched system under moment uncertainty of parameter using Koopman operator*, Optimization, **74**(10) (2025), 1-29. https://doi.org/10.1080/02331934.2025.2588428

[43] Y. Yuan, D. Zhou, J. Li, C. Lou, *Time-varying parameters estimation with adaptive neural network EKF for missile-dual control system*, Journal of Systems Engineering and Electronics, **35**(2) (2024), 451-462. https://doi.org/10.23919/JSEE.2024.000008

[44] L. A. Zadeh, *From computing with numbers to computing with words. From manipulation of measurements to manipulation of perceptions*, IEEE Transactions on Circuits and Systems I: Fundamental Theory and Applications, **46**(1) (1999), 105-119. https://doi.org/10.1109/81.739259

[45] F. Zarei, B. Shafai, *Consensus of multi-agent systems under disturbances using a proportional–integral fading observer*, in International Conference on Integrated Systems: Design and Technology, Springer, 2025. https://doi.org/10.1007/978-3-032-21981-7_7

[46] C. Zhang, J. Hu, J. Qiu, W. Yang, H. Sun, Q. Chen, *A novel fuzzy observer-based steering control approach for path tracking in autonomous vehicles*, IEEE Transactions on Fuzzy Systems, **27**(2) (2018), 278-290. https://doi.org/10.1109/TFUZZ.2018.2856187

[47] F. Zhao, F. Dörfler, A. Chiuso, K. You, *Data-enabled policy optimization for direct adaptive learning of the LQR*, IEEE Transactions on Automatic Control, **70**(11) (2025), 7271-7232. https://doi.org/10.1109/TAC.2025.3569597

[48] N. Zhao, H. Zhang, X. Qiu, R. K. Agarwal, *Observer-based periodic event-triggered adaptive fuzzy control for networked nonlinear systems*, IEEE Transactions on Cybernetics, **55**(7) (2025), 3171-3181. https://doi.org/10.1109/TCYB.2025.3554702

[49] F. Zhu, W. Du, *Observer-based consensus of multi-agent systems under odd distributed impulsive control protocol*, Applied Mathematics and Computation, **466** (2024), 128474. https://doi.org/10.1016/j.amc.2023.128474